

# DETERMINATION AND MINIMIZATION OF CROSS REGULATION IN MULTI-OUTPUT HIGH ORDER SRC

Jai P. Agrawal, K. Siri and C.Q. Lee

Department of Electrical Engineering and Computer Sciences  
University of Illinois at Chicago, P.O.Box 4348,  
Chicago, IL 60680, Tel : (312)996-2664 .

## ABSTRACT

This paper presents the analysis and the technique of determining the cross regulation characteristics in multi-output high order Series Resonant Converters. The steady state cross regulation characteristics are derived using the state-plane techniques, illustrated by the example of a two-output LLC type SRC. It also suggests a technique of minimizing the cross regulation by compensating the differential rate of leakage fluxes in the multiple secondary windings of the isolation transformer. Our theoretical results are verified by simulation.

## I. INTRODUCTION

Most instrument power supplies have more than one output. However, in practice, only one of these outputs is regulated by feedback control, while the others are either unregulated or post regulated. The percentage change in one of the output voltages due to the load variations in other outputs, is known as the cross regulation problem. This problem severely limits the controllability range of each output in the converter.

Most multi-output converters use transformers with multiple secondary windings to deliver power to their loads. The steady state cross regulation in these converters depend on the leakage inductances, the core and the copper losses in their transformers. Previous analytical work on the cross regulation is available mainly in the case of the first order converters such as the buck and the flyback converters. There are studies reported on the second order resonant converters, but none is available for the 3rd or higher order. In this paper, we present an analysis of the cross regulation in multi-output resonant converters of order higher than two. To illustrate our approach, we derive the steady state cross regulation characteristics of a half-bridge two-output LLC type Series Resonant Converter. Based on our analysis, we suggest a technique of minimizing the cross regulation by compensating for the rate of change of differential leakage flux in the secondary windings of the transformer. We use computer simulation to verify our theoretical results.

## II. CONVERTER MODEL FOR A TWO-OUTPUT SRC-LLC

A half-bridge two-output SRC-LLC is given in Fig. 1 and its equivalent circuit is shown in Fig. 2. In the equivalent circuit we use the transformer circuit model [2] in which we assume that the magnetizing inductance,  $L_m$ , is much higher than the leakage inductances of the primary,  $L_{kp}$ , and the two secondary windings,  $L_{k1}$  and  $L_{k2}$ . Therefore,  $L_m$  has been omitted from the equivalent circuit. The primary

leakage inductance  $L_{kp}$  can, however, be included in the resonant inductance  $L_1$ . We have also assumed that the switching frequency is sufficiently low so that the core and the copper losses are negligible and the winding capacitances can be ignored. Furthermore, the resonant inductors  $L_1$  and  $L_2$  are assumed to be much higher than the leakage

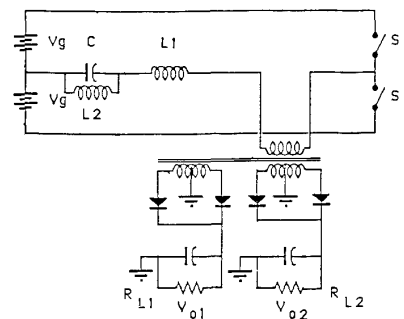


Fig. 1 A half-bridge two-output SRC-LLC

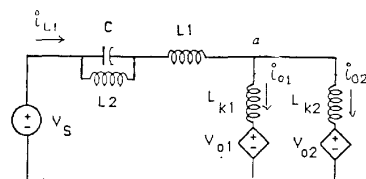


Fig. 2 The equivalent circuit.

inductances.  $V_S$  is an equivalent two-state voltage source  $(+V_g, -V_g)$ , representing the switching inversion in the input circuit. We assume that switches  $S_1$  and  $S_2$  are driven by a square wave of frequency  $f_s$  with 50% duty ratio. The two output circuits consisting of the transformer, rectifiers, filters and the load resistances are modelled as two-state voltage sinks  $V_{E1}$  and  $V_{E2}$  as given below

$$V_{Ei} = \frac{i_{oi}(t)}{|i_{oi}(t)|} V_{oi} \quad i = 1,2 \quad (1)$$

where  $V_{oi}$  and  $i_{oi}$  are the output voltages and currents, respectively. In the following section we present the steady state analysis of the converter in which it is assumed that  $V_{o1}$  is feedback regulated and  $V_{o2}$  is unregulated. It is also assumed that the load current at  $V_{o1}$  is higher than the load current at  $V_{o2}$ .

### III. CONVERTER OPERATION IN CONTINUOUS CONDUCTION MODE

The steady state response of SRC-LLC operating in the continuous conduction mode can be obtained from the converter response of the circuit modes over a half switching period where  $V_S$  equals  $+V_g$ . Consider that in the equivalent circuit of Fig. 2 the currents  $i_{L1}$ ,  $i_{o1}$  and  $i_{o2}$  are all positive. The circuit comprising of  $L_{k1}$ ,  $V_{o1}$ ,  $L_{k2}$  and  $V_{o2}$  can be replaced by an equivalent voltage sink  $V'_o$  in series with an inductor  $L_{ks}$  which are given as

$$V'_o = V_{o1} \frac{L_{k2}}{L_{k1} + L_{k2}} + V_{o2} \frac{L_{k1}}{L_{k1} + L_{k2}} \quad (1)$$

$$L_{ks} = \frac{L_{k1}L_{k2}}{L_{k1} + L_{k2}} \quad (2)$$

The resulting equivalent circuit, given in Fig. 3(a), is used for the analysis of the circuit mode  $m_{11}$  in the converter operation. In this mode, at instant  $t = \tau_3$  the current  $i_{o2}$  becomes zero due to the following condition;

$$V_{o1} + L_{k1} \frac{di_{o1}}{dt} - L_{k2} \frac{di_{o2}}{dt} \leq V_{o2} \quad (3)$$

This will remove  $L_{k2}$  and  $V_{o2}$  out of the circuit of Fig. 2 leaving  $V_{o1}$  as the only effective voltage sink in series with  $L_{k1}$ . The new equivalent circuit is shown in Fig. 3(b) which is used for the analysis of converter operation in the circuit mode  $m_{12}$ . The mode  $m_{12}$  exists until at the instant  $t = t_1$  the inductor current  $i_{L1}$  becomes zero and changes polarity in a resonant manner, causing the polarity inversion of voltage sinks  $V_{o1}$  and  $V_{o2}$ . The current  $i_{o2}$  will also start increasing negatively. Therefore, both voltage sinks and leakage inductances are replaced by  $V'_o$  in series with  $L_{ks}$  as was done in the first circuit mode. The resulting equivalent circuit is shown in Fig. 3(c) which is used for the analysis in circuit mode  $m_{13}$ . The circuit mode  $m_{13}$  exists until the half switching period is over. In the next section, we present the steady state analysis in the above mode sequence by using the state-plane methods.

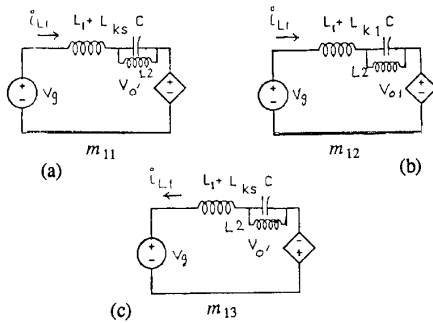


Fig. 3 Circuit modes

#### 3.1 Decomposition of 3rd order circuit modes

It can be seen from Fig. 3 (a) that each circuit mode is a 3rd order circuit. Before the state-plane methods can be applied, each circuit mode is decomposed into a first order circuit and a 2nd order resonant circuit by using the technique presented in [3]. Consider circuit mode  $m_{11}$  shown in Fig. 3(a). It can be shown that in the s-domain, the inductor current  $i_{L1}$  and the capacitor voltage  $v_c$  are given as follows,

$$\begin{bmatrix} i_{L1}(s) \\ V_C(s) \end{bmatrix} = \begin{bmatrix} \frac{s^2 + \omega_2^2}{(L_1 + L_{ks})s^2(s^2 + \omega_{01}^2)} \\ \frac{\omega_1^2}{s(s^2 + \omega_{01}^2)} \end{bmatrix} (V_S - V_E) \quad (4)$$

where,

$$\omega_1^2 = \frac{1}{(L_1 + L_{ks})C}, \quad \omega_2^2 = \frac{1}{L_2C}, \quad \omega_{01}^2 = \frac{L_1 + L_{ks} + L_2}{(L_1 + L_{ks})L_2C}$$

By expanding eq. (1) into partial fractions, we obtain

$$\begin{bmatrix} i_{L1}(s) \\ V_C(s) \end{bmatrix} = \frac{1}{s^2} \begin{bmatrix} 0 & 1 \\ 1 & 0 \end{bmatrix} \begin{bmatrix} 0 \\ (V_S - V_E) \end{bmatrix} + \frac{1}{s^2 + \omega_{01}^2} \begin{bmatrix} 0 & 1 \\ 1 & -s \end{bmatrix} \begin{bmatrix} 0 \\ (V_S - V_E) \frac{L_2}{L_1 + L_{ks} + L_2} \end{bmatrix} \quad (5)$$

From eqn.(5) we can synthesize a first order and a second order circuit as shown in Fig. 4(a)

$$i_{L1} = i_{s0} + i_{s1} \quad (6)$$

$$b_1 = \frac{L_2}{L_1 + L_2 + L_{ks}} \quad (7)$$

The decomposed circuits for all circuit modes in are shown in Fig. 4 (a),(b) and (c), where,

$$b_2 = \frac{L_2}{L_1 + L_2 + L_{k1}} \quad (8)$$

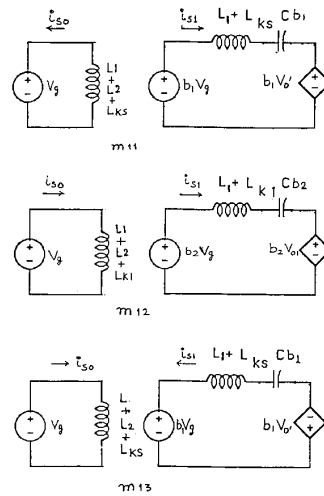


Fig. 4 The decomposed circuit modes in sequence 1.

#### 3.2 State-plane Analysis

In the state-plane analysis, we normalize all voltages and currents with respect to  $V_g$  and  $V_g/Z_{01j}$ , respectively, where  $Z_{01j}$  is the characteristic impedance of circuit mode  $m_{1j}$ . Furthermore, the converter gains  $M_1$  and  $M_2$  are used in place of the normalized output voltages  $V_{no1}$  and  $V_{no2}$ .

The state-plane trajectory for the first order circuit, shown in Fig. 5, consists of straight line segments. The state-plane trajectory of the resonant circuit for a circuit mode consists of circular arc as shown in Fig. 6. The normalized state-plane equation is given by,

$$\frac{di_{ns1}}{dv_{nc1}} = \frac{-v_{nc1} + b(1 - V_{nE})}{i_{ns1}} \quad (9)$$

where  $b$  is a constant in a specific circuit mode. The singular point on the normalized state-plane is  $[b(1 - V_{nE}), 0]$ .

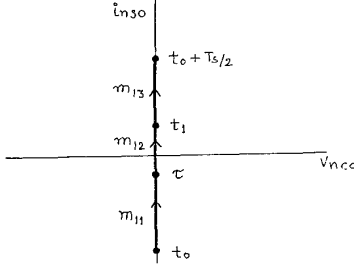


Fig. 5 The state-plane trajectory of the First order circuit modes in Sequence 1.

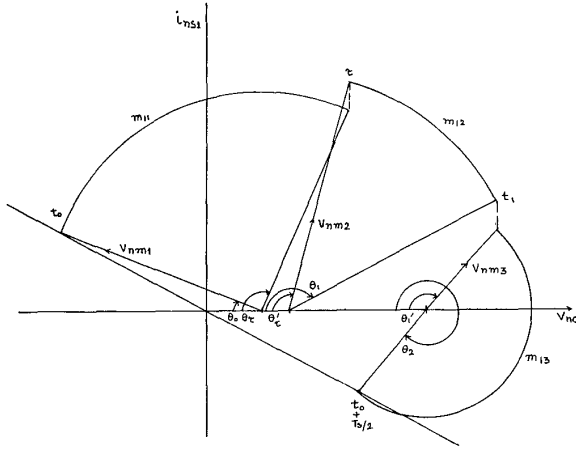


Fig. 6 The state-plane trajectory of the 2nd order circuit modes in Sequence 2.

The current  $i_{nL1}$  in a circuit mode  $m_{11}$  is obtained from

$$i_{nL} = i_{ns0} + i_{ns1} \quad (10)$$

Fig. 7 shows the analytically predicted waveforms of currents  $i_{L1}(t)$ ,  $i_{o1}(t)$  and  $i_{o2}(t)$

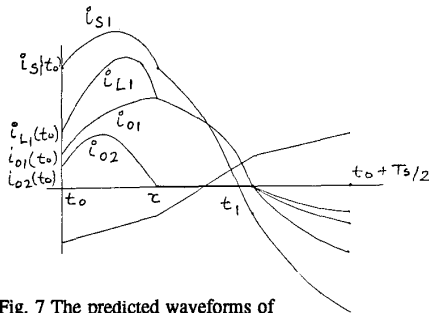


Fig. 7 The predicted waveforms of  $i_{L1}(t)$ ,  $i_{o1}(t)$  and  $i_{o2}(t)$ .

The normalized average current  $I_{no2}$  which is supplied to the load  $R_{L2}$ , can be obtained from averaging  $i_{no2}$  over the half switching period in sequence 1, which is given by

$$\begin{aligned} I_{no2} &= \frac{M_2}{Q_2} = \frac{f_{ns}}{\pi} \left[ \int_{\theta_0}^{\theta_c} i_{no2} d\theta - \int_{\theta_1}^{\theta_2} i_{no2} d\theta \right] \quad (11) \\ &= \frac{f_{ns}}{\pi} \left\{ (\theta_c - \theta_0) \left[ i_{no2}(t_0) - \frac{a}{a+1} i_{ns1}(t_0) \right] \right. \\ &\quad + \frac{a(k_1+1)}{2(a+1)^2} (M_1 - M_2) [(\theta_c - \theta_0)^2 - (\theta_2 - \theta_1')^2] \\ &\quad + \frac{a}{2(a+1)(k_1+k_2+1)} [(1 - V'_{no})(\theta_c - \theta_0)^2 + (1 + V'_{no})(\theta_2 - \theta_1')^2] \\ &\quad + \frac{a}{a+1} [V_{nm1}(\cos \theta_0 - \cos \theta_c) - V_{nm3}(\cos \theta_1' - \cos \theta_2)] \\ &\quad \left. - \frac{a}{a+1} [i_{ns1}(t_0)(\theta_c - \theta_0) - V_{nm3} \sin \theta_1' (\theta_2 - \theta_1')] \right\} \quad (12) \end{aligned}$$

where,

$$k_1 = \frac{L_1}{L_{ks}}, \quad k_2 = \frac{L_2}{L_{ks}}, \quad a = \frac{L_{k1}}{L_{k2}}$$

The normalized average current  $I_{ng}$  supplied by the source can be obtained from averaging  $i_{nL1}(t)$  over the half switching period, which is given by

$$\begin{aligned} I_{ng} &= \frac{f_{ns}}{\pi} \left[ \int_{\theta_0}^{\theta_c} i_{nL1} d\theta + \int_{\theta_c}^{\theta_1} \frac{Z_{011}}{Z_{012}} i_{nL1} d\theta + \int_{\theta_1}^{\theta_2} i_{nL1} d\theta \right] \quad (13) \\ &= \frac{f_{ns}}{\pi} \left\{ i_{ns0}(t_0)(\theta_c - \theta_0) + \frac{k_1+1}{2(k_1+k_2+1)} (1 - V'_{no})(\theta_c - \theta_0)^2 \right. \\ &\quad + (1 + V'_{no})(\theta_2 - \theta_1')^2 + V_{nm1}(\cos \theta_0 - \cos \theta_c) \\ &\quad + \frac{Z_{011}}{Z_{012}} (i_{ns0}(\tau)(\theta_1 - \theta_c) + \frac{k_1+a+1}{2(k_1+k_2+a+1)} (1 - M_1)(\theta_1 - \theta_c)^2 \\ &\quad + V_{nm2}(\cos \theta_c - \cos \theta_1)) + i_{ns0}(t_1)(\theta_2 - \theta_1') \\ &\quad \left. + V_{nm3}(\cos \theta_1' - \cos \theta_2) \right\} \quad (14) \end{aligned}$$

#### IV. CROSS REGULATION CHARACTERISTICS

By equating the power supplied from the source to the power delivered to the load, we obtain

$$I_{ng} = \frac{M_1^2}{Q_1} + \frac{M_2^2}{Q_2} \quad (15)$$

where  $Q_1$  and  $Q_2$  are the normalized load resistances of  $R_{L1}$  and  $R_{L2}$  with respect to  $Z_{011}$ , respectively. From the steady state solution of both sequences in the previous section, the converter gain  $M_2$  can be derived as a function of  $Q_1$ ,  $Q_2$  and  $M_1$ . The cross regulation characteristics are plotted as the curves of  $M_2/M_1$  vs.  $Q_1/Q_2$  with  $M_1$  and

$L_{k1}/L_{k2}$  as parameters. Fig. 8 shows the curves for SRC-LLC operating in the continuous conduction mode. The cross regulation of second output can be obtained from the slope of the characteristic curves. A lower slope indicates a lower cross regulation. The cross regulation for  $L_{k1}/L_{k2} = 0.33$  is higher than that for the case of  $L_{k1}/L_{k2} = 3.0$ . The cross regulation is expected to be the best at  $L_{k1}/L_{k2} = 1.0$ .

The characteristics curves with  $M_1$  as parameter in Fig. 8(b) show that the cross regulation is lower for a lower value of converter gain  $M_1$ . Low converter gain  $M_1$  is a desirable feature for good self-regulation [1] in SRC topologies. This will allow for the use of a low turn ratio high frequency transformer in the converter design. Furthermore, the cross regulation in SRC-LLC is much lower than that reported in [2] for the case of a 2nd order SRC-CVC case.

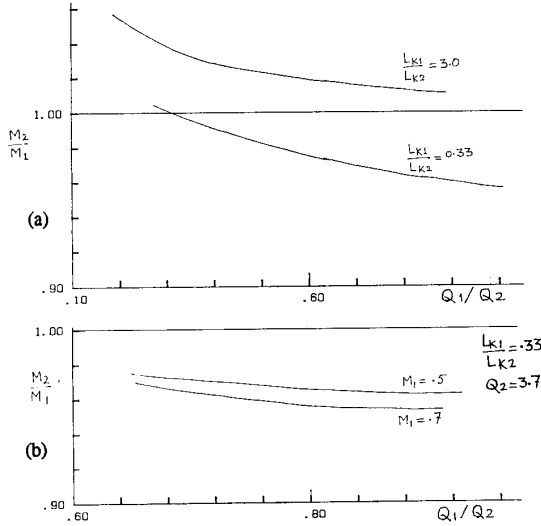


Fig. 8 The Cross Regulation Characteristics of LLC-SRC.

## V. MINIMIZATION OF CROSS REGULATION

It can be shown from the converter equivalent circuit shown in Fig. 2 that the difference in the two output voltages is due to the rate of change of the differential leakage flux in the two secondary windings;

$$V_{o2} - V_{o1} = L_{k1} \frac{di_{o1}}{dt} - L_{k2} \frac{di_{o2}}{dt} \quad (16)$$

$$= \frac{d}{dt} (\phi_{k1} - \phi_{k2}) \quad (17)$$

where the leakage fluxes in the transformer secondary windings are given by,  $\phi_{ki} = L_{ki} i_{oi}$   $i = 1, 2$  (18)

The differential rate of change of leakage flux can be compensated by connecting an additional transformer as shown in Fig. 9. The transformer has 1:1 turn ratio. In this technique, the output currents are forced to become zero simultaneously. A high capacitor value of  $C_{o1}$  and  $C_{o2}$  are added in series with the transformer provide the isolation between the two output circuits

## VI. SIMULATION RESULTS

A two-output converter circuit was simulated using MCAPII program which has following parameters:

$V_g = 75$  V,  $L_{k1} = 1$   $\mu$ H,  $L_{k2} = 3$   $\mu$ H,  $L_1 = L_2 = 12$   $\mu$ H,  $C = 33$  nF  
Switching frequency = 312.5 KHz, Resonant frequency = 359 KHz

Fig. 10 shows the waveforms of  $i_{L1}$ ,  $i_{o1}$  and  $i_{o2}$  for converter gains of  $M_1 = 0.61$ , and  $M_2 = 0.63$ , with loads  $R_{L1} = 20$  ohms and  $R_{L2} = 100$  ohms, are in full agreement with the analytical waveforms. The experimental verification of above results along with the implementation of the minimization technique will be presented in a future paper.

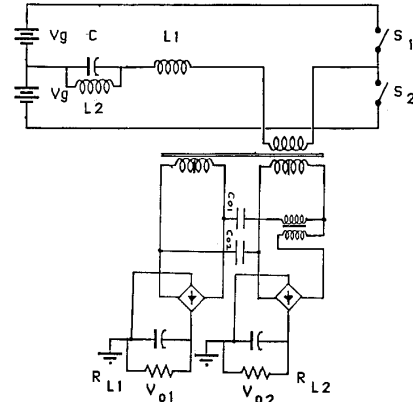


Fig. 9 The cross regulation minimization by compensating the differential rate of leakage fluxes in the transformer secondary

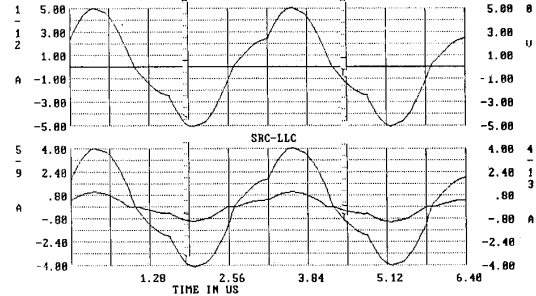


Fig. 10 The simulated current waveforms in LLC-SRC circuit.

## VII. CONCLUSION

The cross regulation characteristics are as useful as the self-regulation characteristics in the converter design. In this paper we have analyzed the steady state operation of a two-output SRC-LLC in continuous conduction mode and derived the cross regulation characteristics. A technique has been suggested to minimize cross regulation by incorporating an extra transformer to compensate for the differential rate of leakage fluxes in the main transformer. The analytically predicted waveforms are verified by computer simulation.

## Reference

- [1] Rui Liu and C.Q.Lee, "The LLC-type Series Resonant Converter — Variable Switching Frequency Control", Proc. 32nd Midwest Symposium on Circuits and Systems, Urbana, Illinois, Aug. 1989.
- [2] J.P.Agrawal and C.Q.Lee, "Determination of Cross Regulation in Multi-output Resonant Converters", to be presented at APEC 90, Los Angeles, U.S.A.
- [3] J.P.Agrawal, C.Q.Lee, "Decomposition of Circuit Modes in High Order Resonant Converters", Proc. Midwest Symposium on Circuits and Systems, Urbana, Illinois, Aug. 1989.